



HAL
open science

Evaluation of the Energy Efficiency of a Fleet of Electric Vehicle for Eco-Driving Application

W. Dib, A. Chasse, D. Di Domenico, P. Moulin, A. Sciarretta

► **To cite this version:**

W. Dib, A. Chasse, D. Di Domenico, P. Moulin, A. Sciarretta. Evaluation of the Energy Efficiency of a Fleet of Electric Vehicle for Eco-Driving Application. *Oil & Gas Science and Technology - Revue d'IFP Energies nouvelles*, 2012, 67 (4), pp.589-599. 10.2516/ogst/2012023 . hal-01936514

HAL Id: hal-01936514

<https://ifp.hal.science/hal-01936514>

Submitted on 2 Jan 2019

HAL is a multi-disciplinary open access archive for the deposit and dissemination of scientific research documents, whether they are published or not. The documents may come from teaching and research institutions in France or abroad, or from public or private research centers.

L'archive ouverte pluridisciplinaire **HAL**, est destinée au dépôt et à la diffusion de documents scientifiques de niveau recherche, publiés ou non, émanant des établissements d'enseignement et de recherche français ou étrangers, des laboratoires publics ou privés.



This paper is a part of the hereunder thematic dossier published in *OGST Journal*, Vol. 67, No. 4, pp. 539-645 and available online [here](#)

Cet article fait partie du dossier thématique ci-dessous publié dans la revue *OGST*, Vol. 67, n°4, pp. 539-645 et téléchargeable [ici](#)

DOSSIER Edited by/Sous la direction de : **A. Sciarretta**

Electronic Intelligence in Vehicles Intelligence électronique dans les véhicules

Oil & Gas Science and Technology – Rev. IFP Energies nouvelles, Vol. 67 (2012), No. 4, pp. 539-645

Copyright © 2012, IFP Energies nouvelles

- 539 > Editorial
- 547 > *Design and Optimization of Future Hybrid and Electric Propulsion Systems: An Advanced Tool Integrated in a Complete Workflow to Study Electric Devices*
Développement et optimisation des futurs systèmes de propulsion hybride et électrique : un outil avancé et intégré dans une chaîne complète dédiée à l'étude des composants électriques
F. Le Berr, A. Abdelli, D.-M. Postariu and R. Benlamine
- 563 > *Sizing Stack and Battery of a Fuel Cell Hybrid Distribution Truck*
Dimensionnement pile et batterie d'un camion hybride à pile à combustible de distribution
E. Tazelaar, Y. Shen, P.A. Veenhuizen, T. Hofman and P.P.J. van den Bosch
- 575 > *Intelligent Energy Management for Plug-in Hybrid Electric Vehicles: The Role of ITS Infrastructure in Vehicle Electrification*
Gestion énergétique intelligente pour véhicules électriques hybrides rechargeables : rôle de l'infrastructure de systèmes de transport intelligents (STI) dans l'électrification des véhicules
V. Marano, G. Rizzoni, P. Tulpule, Q. Gong and H. Khayyam
- 589 > *Evaluation of the Energy Efficiency of a Fleet of Electric Vehicle for Eco-Driving Application*
Évaluation de l'efficacité énergétique d'une flotte de véhicules électriques dédiée à une application d'éco-conduite
W. Dib, A. Chasse, D. Di Domenico, P. Moulin and A. Sciarretta
- 601 > *On the Optimal Thermal Management of Hybrid-Electric Vehicles with Heat Recovery Systems*
Sur le thermo-management optimal d'un véhicule électrique hybride avec un système de récupération de chaleur
F. Merz, A. Sciarretta, J.-C. Dabadie and L. Serrao
- 613 > *Estimator for Charge Acceptance of Lead Acid Batteries*
Estimateur d'acceptance de charge des batteries Pb-acide
U. Christen, P. Romano and E. Karden
- 633 > *Automatic-Control Challenges in Future Urban Vehicles: A Blend of Chassis, Energy and Networking Management*
Les défis de la commande automatique dans les futurs véhicules urbains : un mélange de gestion de châssis, d'énergie et du réseau
S.M. Savaresi

Evaluation of the Energy Efficiency of a Fleet of Electric Vehicle for Eco-Driving Application

W. Dib*, A. Chasse, D. Di Domenico, P. Moulin and A. Sciarretta

IFP Energies Nouvelles, 1-4 avenue de Bois-Préau, 92852 Rueil-Malmaison Cedex - France
e-mail: wissam.dib@ifpen.fr - alexandre.chasse@ifpen.fr - domenico.didomenico@ifpen.fr - philippe.moulin@ifpen.fr - antonio.sciarretta@ifpen.fr

* Corresponding author

Résumé — Évaluation de l'efficacité énergétique d'une flotte de véhicules électriques dédiée à une application d'éco-conduite — Dans cet article, nous proposons une approche pour évaluer l'efficacité énergétique d'un véhicule électrique lors d'un déplacement urbain. Cette approche fournit des outils permettant d'évaluer le gain énergétique réalisable par l'intermédiaire des techniques intelligentes d'éco-conduite. Cette approche peut être utilisée pour évaluer une flotte de véhicules, ainsi que pour élaborer une cartographie énergétique d'une ville. Des données expérimentales sont fournies pour illustrer cette approche sur une flotte de véhicules électriques dans un environnement urbain. Les méthodes d'éco-conduite proposées sont destinées à constituer la base d'un système d'assistance au conducteur.

Abstract — Evaluation of the Energy Efficiency of a Fleet of Electric Vehicle for Eco-Driving Application — In this paper, an approach to evaluate the energy efficiency of an electrical vehicle during a short trip is addressed. This approach provides metrics that can be used to evaluate the potential of improvement achievable via intelligent eco-driving techniques and the performance actually achieved by any of them. It can be the basis for an evaluation of a fleet of vehicles and of a whole city for which an energy efficiency map could be derived, depending for instance of traffic management strategy. Experimental data are provided to illustrate the approach for a fleet of electric vehicles in an urban environment. The methods proposed are intended to be the basis of a driver assistance system oriented to optimal eco-driving.

INTRODUCTION

In recent years, environmental issues such as energy saving and reduction of CO₂ emission are emphasized. In particular, the energy consumption of automobiles accounts for a substantial amount of all transportation sectors. There are various approaches to reduce the fuel consumption of automobiles. For this purpose, high efficient powertrain and lightweight automobiles are being developed. On the other hand, the so-called “eco-driving” can also reduce the fuel consumption.

Eco-driving is now considered to be a major way of reducing the energy consumption linked to the transport of people or goods. However, the meaning of this expression is not very clear and encompasses different concepts. Generally, the idea is that there are different ways of driving a specific journey that are not equivalent from an energy point of view. Eventually, the objective is to find the optimal one.

More generally, for personal cars, many features are proposed or will be proposed in the near future by car manufacturers. Most of the time, they consist of advising the driver

to change gear or to adopt a moderate velocity [1], through an interface integrated in the dash boards of vehicles. In this case, the approach is mainly static: only the choice of the engine operating point is considered and the speed trajectory is neglected. In effect, the energy (or fuel) consumption is reduced but there is no guarantee that the driving behavior is optimal. The assessment of this kind of features is not addressed (to the authors knowledge).

In this context, several studies that investigate the problem of optimization of the speed trajectory of the vehicle have been reported [2-4]. The goal of vehicle trajectory control is to determine which is the vehicle speed profile that minimizes the fuel consumption over a given time horizon, usually with various constraints that depend on the particular route [5]. Therefore, for heavy trucks or for trains, control strategies have been proposed to optimize the vehicle speed trajectory on motorways [6] and have already shown that the fuel consumption can be significantly reduced.

In this paper, we propose an approach to evaluate the energy efficiency of a travel of a vehicle. This approach provides metrics that can be used to evaluate the potential of improvement achievable *via* eco-driving techniques and the performance actually achieved by any of them. It can be the basis for an evaluation of a fleet of vehicles and of a whole city for which an energy efficiency map could be derived, depending for instance of traffic management strategy. Experimental data are provided to illustrate the approach for a fleet of electric vehicles in an urban environment. The methods proposed are intended to be the basis of a driver-assistance system oriented to optimal eco-driving.

The structure of the paper is as follows. Section 1 presents the mathematical model of the vehicle system and its identification using experimental data. Then, the optimization problem is formulated in Section 2. In Section 3, we show the experimental illustration. Finally, we wrap up the paper with some concluding remarks.

1 SYSTEM MODELING

The vehicle is a small electric car propelled by a AC traction motor, connected to the rear wheels by a fixed reduction gear. A battery pack provides power to the motor through a DC/AC converter. The vehicle can be modeled as a standard drive-train as seen in the schematic in Figure 1, including the battery, auxiliary losses, DC/ AC converter and the electric motor.

The vehicle model used here is a basic longitudinal model that captures the inertial dynamics of the vehicle and the efficiency of the powertrain components, to be able to predict energy consumption. The foundation for the modeling work can be found in [7]. This section illustrates how the model is built and validated using the information provided by some external measurements on the vehicle. Different experimental tests have been done on the vehicle for this purpose. Note

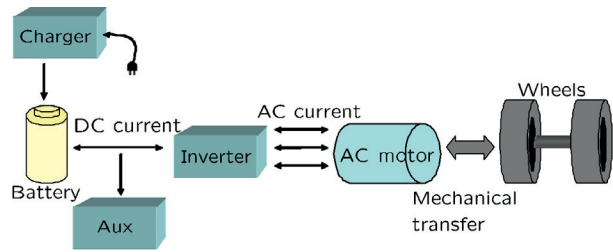


Figure 1

F-CITY drive train schematic.

that the information given by the vehicle manufacturer does not include any detailed characterization of the components of the vehicle (F-CITY). These data are shown in Table 1.

TABLE 1
F-CITY datasheet

Performance		
Maximum speed	65 km/h	
Range	80 to 100 km	
Acceleration from 0 to 30 km/h	5.5 s	
Electrical components		
	Type	Power
Motor	AC	8 kW /11 hp
Battery	Ni-MH	14.4 kWh
Maximum weight		
	1 140 kg	

1.1 Vehicle Model

The motion of the vehicle is governed by the usual longitudinal dynamics model:

$$M \frac{dv}{dt} = F_t - F_{res} - F_{slope} - F_{brk} \quad (1)$$

where M is the total mass of the vehicle, v is the speed of the vehicle, F_t is the traction force, F_{res} is the resistive force that summarizes the aerodynamic friction and the rolling friction, F_{slope} is the force caused by gravity, and F_{brk} is the mechanical brake force, respectively. F_{res} can be expressed as:

$$F_{res} = a + bv + cv^2 \quad (2)$$

where a , b and c are parameters to be identified. Finally F_{slope} can be modeled as:

$$F_{slope} = Mgsin(\alpha) \quad (3)$$

where α is the road slope and g is the gravitational acceleration.

1.2 Electrical Components

1.2.1 AC Motor

The traction motor is a AC motor. The data provided does not include a steady-state map of the electric power nor an efficiency map but only few measurements of armature voltage, current, speed and power on some steady state operating points. Therefore, in order to identify the following steady state map:

$$P_{elec} = \phi_{elec}(T_{mot}, \omega_{mot}) \quad (4)$$

we use a dynamical model of the motor and we develop a control law to track the requested torque. Thus, the voltage equations are given by:

$$\begin{aligned} V_{ds} &= R_s I_{ds} - \omega_s \phi_{qs} + \frac{d\phi_{ds}}{dt} \\ V_{qs} &= R_s I_{qs} + \omega_s \phi_{ds} + \frac{d\phi_{qs}}{dt} \\ 0 &= R_r I_{dr} - \omega_r \phi_{qr} + \frac{d\phi_{dr}}{dt} \\ 0 &= R_r I_{qr} + \omega_r \phi_{dr} + \frac{d\phi_{qr}}{dt} \end{aligned} \quad (5)$$

where the stator and rotor flux linkages are defined using their respective self leakage inductances and mutual inductance as given below:

$$\begin{aligned} \phi_{ds} &= L_s I_{ds} + M I_{dr} \\ \phi_{qs} &= L_s I_{qs} + M I_{qr} \\ \phi_{dr} &= L_r I_{dr} + M I_{ds} \\ \phi_{qr} &= L_r I_{qr} + M I_{qs} \end{aligned} \quad (6)$$

The stator and rotor resistance (R_s, R_r), the stator and rotor inductance (L_s, L_r), as the mutual inductance M are parameters to be identified. The motor speed is computed as:

$$\omega_{mot} = \omega_s - \omega_r \quad (7)$$

Finally the electromagnetic torque and the power consumed by the motor are given by:

$$T_{mot} = p \frac{M}{L_r} (\phi_{dr} I_{qs} - \phi_{qr} I_{ds}) \quad (8)$$

$$P_{elec} = V_{ds} I_{ds} + V_{qs} I_{qs} + V_{dr} I_{dr} + V_{qr} I_{qr} \quad (9)$$

To track the torque of this machine, we have developed a model based control law where the control actions are the voltages and the frequency of the machine. This control law can be summarized by:

$$(V_{ds}, V_{qs}, \omega_s) = \psi(T_{mot}, \omega_{mot}) \quad (10)$$

Due to space limitations, we have omitted the mathematical proof and the development of this controller. See [8] for more details.

1.2.2 Battery Model

The battery is described by a simple equivalent circuit:

$$U_{bat} = E(\xi) - R(\xi) I_{bat} \quad (11)$$

which explicitly relates the battery voltage U_{bat} to its current I_{bat} . The voltage source E and the resistance R are varying with the state of charge ξ . Assuming that the auxiliary power consumed is zero then the net electrochemical power (*i.e.* the one that corresponds to the actual battery charge or discharge) can be expressed as:

$$P_{bat} = E I_{bat} \quad (12)$$

where:

$$I_{bat} = \frac{E}{2R} - \sqrt{\frac{E^2 - 4P_{elec}R}{4R^2}} \quad (13)$$

1.3 Use of the Model and Input Variable

This model is used in either forward or backward mode. The forward mode reproduces the physical causality of the system, *i.e.* the model is used to compute the vehicle acceleration given the control inputs (position of the acceleration and brake pedals). The backward mode instead is used to compute the power consumption of a given speed profile which is the principal input of the model. In this case, the resulting torque demand $T_{pwt,sp}$ can be positive (traction) or negative (braking). The requested motor torque T_{mot} is then determined as:

$$T_{pwt,sp} = F_t R_{tyre} = T_{mot} R_1 \eta_{trans} \quad (14)$$

where R_1 is the constant motor-to-wheels transmission ratio, R_{tyre} is the radius of the wheel and η_{trans} is the transmission efficiency. This application of the model in the backward mode allows to process the experimental data available in order to obtain the corresponding estimate of power and energy consumption.

The forward model, on the other hand, is used for the simulations to predict the vehicle speed given T_{pwt} and F_{brk} . Both these quantities are determined by the single control variable u , a non dimensional quantity varying in the interval $[-1, 1]$. Values of u smaller than $u_{mech,brk}$ correspond to the use of mechanical brakes ($F_{brk} > 0$) while values larger than $u_{mech,brk}$ modulate the electric motor between its minimum and maximum current. In formulas:

$$T_{pwt}(u) = T_{pwt,min} + u^+ (T_{pwt,max} - T_{pwt,min}) \quad (15)$$

$$F_{brk}(u) = u^- F_{brk,max} \quad (16)$$

where:

$$u^+ = \begin{cases} u & \text{if } u \geq u_{mech,brk} \\ 0 & \text{if } u < u_{mech,brk} \end{cases} \quad \text{and} \quad u^- = \begin{cases} 0 & \text{if } u \geq u_{mech,brk} \\ -u & \text{if } u < u_{mech,brk} \end{cases}$$

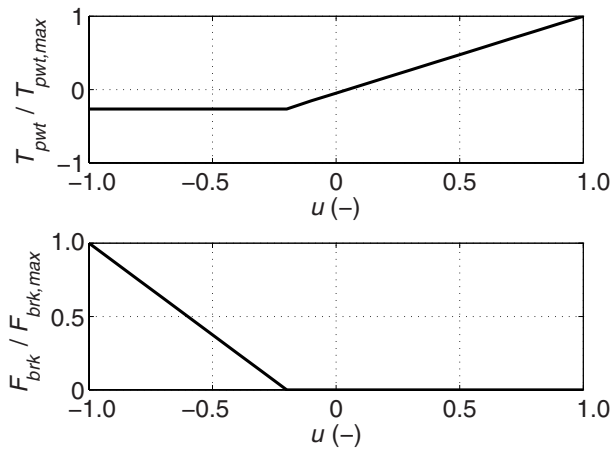


Figure 2

Representation of $T_{pwt}(u)$ and $F_{brk}(u)$.

See Figure 2 for a graphical representation of these formulas.

The value $u = u_{mech,brk}$ corresponds to the minimum motor torque, which is negative and generates the maximum regenerative braking $T_{pwt,min}$. The latter and $u_{mech,brk}$ are also identified due to some experimental tests. Note that $T_{pwt,max}$ corresponds to the maximum motor torque applied on the powertrain and $F_{brk,max}$ to the maximum braking force, respectively.

1.4 Model Identification

Based on the model defined above, the following parameters are identified using experimental measurements:

- the parameters related to the longitudinal vehicle, a, b, c ;
- the parameters of the electric motor, R_s, R_r, L_s, L_r, M ;
- the voltage source of the battery function of the state of charge, $E(\xi)$ and its internal resistance $R(\xi)$;
- and the values of $u_{mech,brk}$ and $T_{pwt,min}$.

The identification of these parameters can be done separately with the measurements provided on the vehicle.

1.4.1 Vehicle Parameters

The vehicle parameters a , b and c in Equations (1) and (2) are obtained by minimizing the error:

$$\epsilon_v = \sum_{l \in \text{decel}} \left| \frac{M dv}{dt}(l) - a - bv(l) - cv^2(l) \right| \quad (17)$$

during deceleration phase ($F_t = 0$) and on a flat road ($F_{slope} = 0$). The index l represents the discretization step of the measurements. The results of the fitting are shown in Figure 3. By doing this, we get $a = 137.4773$ N, $b = 6.4275 \frac{\text{N}}{\text{m/s}}$ and $c = 0.4763 \frac{\text{N}}{(\text{m/s})^2}$. Figure 4 shows the resistive power computed from the vehicle model identified

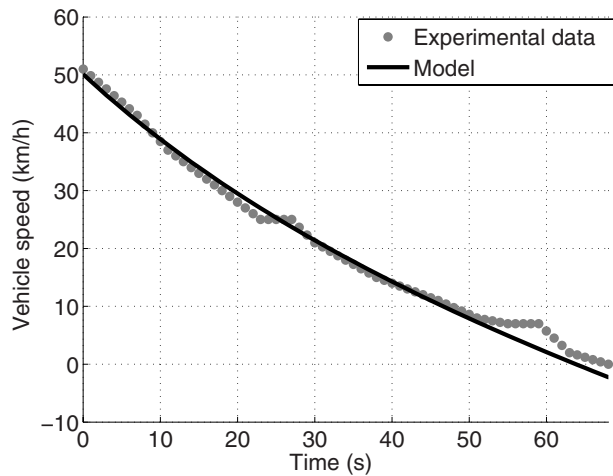


Figure 3

Curve-fitting of the vehicle parameters.

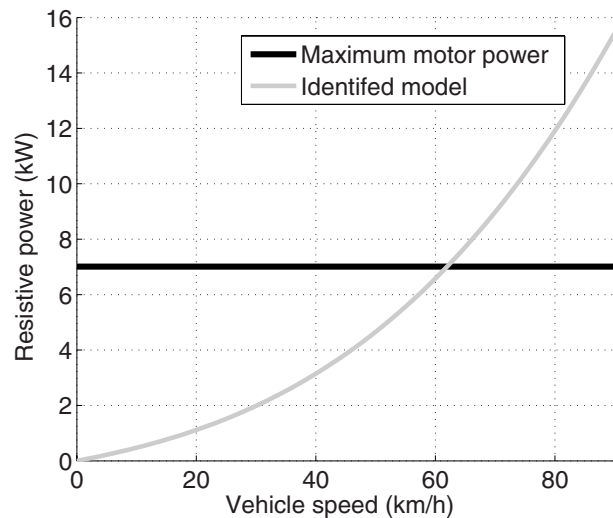


Figure 4

Resistive power versus the vehicle speed.

above with the maximum motor power given by the vehicle manufacturer function of the speed. As we can see, the maximum speed (the intersection between the two curves) is around 63 km/h which is compatible with the one given in the datasheet of the vehicle.

1.4.2 Motor Parameters

By means of the measurements provided from the vehicle, we identify the following information concerning the motor:

- the motor should ensure more than 8 kW for a motor speed 6 200 rpm in a static phase;
- and more than 60 Nm and 15 kW as mechanical power transiently.

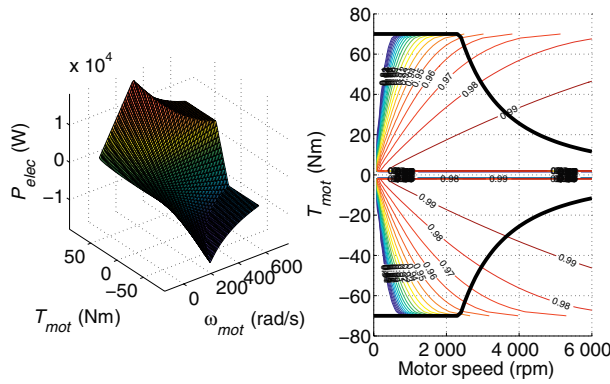


Figure 5
Steady state map of the electric power of the motor.

Based on these constraints combined with the datasheet of the motor given by the vehicle manufacturer, we identify the different parameters of the motor using the dynamical model defined above. Therefore we get $R_s = 0.00431 \Omega$, $R_r = 0.00431 \Omega$, $L_s = 0.017 \text{ H}$, $L_r = 0.017 \text{ H}$, $M = 0.016869 \text{ H}$. See [9] for more details. Therefore, combining the dynamical motor model identified with its model based controller, we identify the steady state map of the electric power and the efficiency as depicted in Figure 5.

1.4.3 Battery Parameters

Using Equations (11) and (13), the battery parameters can be found minimizing:

$$\epsilon_b = \frac{\sum_l |U_{bat}(l) - \hat{U}_{bat}(l)|}{\sum_l |U_{bat}(l) - (E(\xi) - R(\xi)I_{bat}(l))|} \quad (18)$$

where $(\hat{\cdot})$ defines the estimated value. To do that and due to the lack of experimental measurement, we proceed by two steps. First, we identify $E(\xi)$ in the relaxation phase where $I_{bat} = 0$, then we identify $R(\xi)$. Figures 6 and 7 show the identified variables versus the state of charge of the battery (ξ).

1.4.4 Identification of $u_{mech,brk}$ and $T_{pwt,min}$

As shown in Figure 2, $u = u_{mech,brk}$ corresponds to the minimum motor torque, which is negative and generates the maximum regenerative braking $T_{pwt,min}$. Moreover for $u = 0$, the motor torque is also not zero. To identify $T_{pwt,min}$ let us first define the mechanical brake power as:

$$P_{brake}(v) = \min(a_{brk} + b_{brk}v(t), P_{brake}^{max}) \quad (19)$$

Minimizing:

$$\epsilon_{brk} = \sum_{l \in \text{decel}} \left| M \frac{dv}{dt}(l) - M \frac{\hat{dv}}{dt}(l) \right| \quad (20)$$

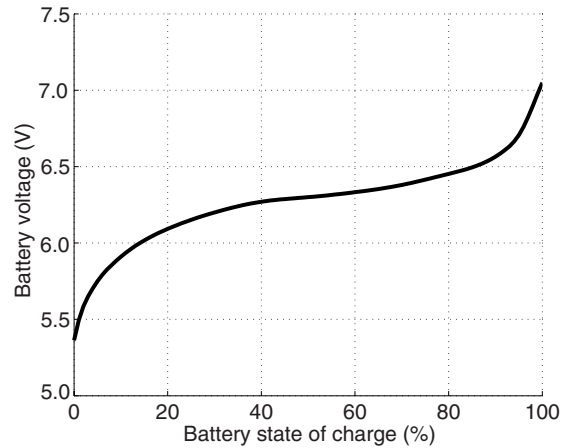


Figure 6
Battery voltage source versus the state of charge.

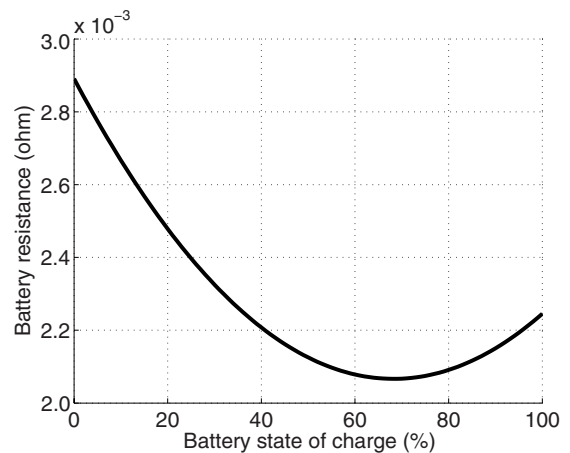


Figure 7
Battery resistance versus the state of charge.

with:

$$M \frac{\hat{dv}}{dt} = \frac{P_{brake}(v(l))}{v(l)} - a - bv(l) - cv^2(l) \quad (21)$$

during the deceleration and braking phase, we can observe the following features (Fig. 8):

- below a given speed threshold $\bar{\omega}_{mot} = 3700 \text{ rpm}$ the maximum regenerative motor torque is constant and is equal to 16.8 Nm;
- above $\omega_{mot} > \bar{\omega}_{mot}$, the motor has a mechanical power limitation defined by $P_{brake}^{max} = 6.6 \text{ kW}$.

Therefore using Equation (14), we can easily compute $T_{pwt,min}$. Following the same procedure, we can identify the motor torque for $u = 0$. This leads to $u_{mech,brk} = -0.2$.

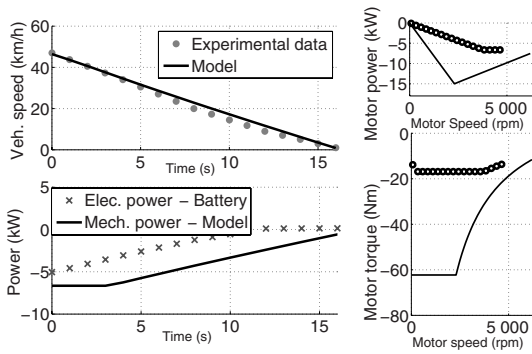


Figure 8

Validation of the complete vehicle model.

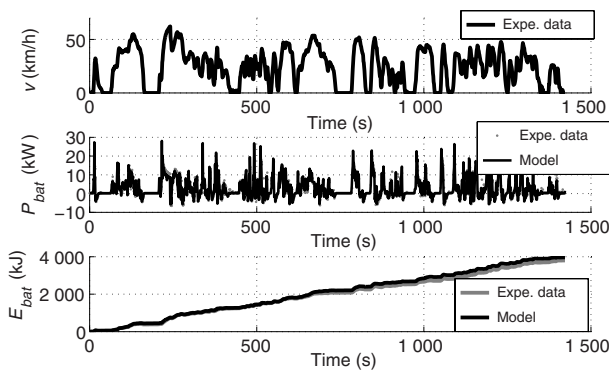


Figure 9

Validation of the complete vehicle model.

1.5 Overall Model Validation

Using the vehicle model identified above in the backward mode, we compute the power and the energy of the battery for a given vehicle speed acquisition. On the other hand, we compute the measured battery energy, as calculated from the experimental data:

$$E_{bat} = \sum_1^k (U_{bat}(l) \cdot I_{bat}(l)) \Delta t$$

and we compare to the model output. See Figure 9.

Conclusion on validation. On the basis of the results shown, the model proposed is deemed sufficiently accurate to represent the vehicle behavior from a system-level point of view, where the model overall error is less than 1.7% over 10 km of traveled distance. This error is basically due to the lack of an accurate measurement of the road slope, the fact

that we use a simple model for the losses in the electrical motor and finally, due to wind force.

2 METRICS FOR ECO-DRIVING EVALUATION

2.1 Eco-Driving Indicator

The objective of this section is to propose an indicator to evaluate the potential of improvement achievable *via* eco-driving techniques and the performance actually achieved by any of these techniques.

To do that, we propose to compare the overall energy consumption of the vehicle during a road trip in a real-life driving conditions, with the minimum energy consumption that is necessary to complete the trip. The latter is calculated by means of the speed profile optimization that will be discussed in the next section. The ‘eco-driving’ indicator can be explicitly defined as:

$$ECO_{Energy} = \frac{E_{bat,opt}}{E_{bat,nom}} \quad (22)$$

where $E_{bat,nom}$ is the energy consumption of the battery for the *nominal* case, *i.e.* under real-life driving conditions and $E_{bat,opt}$ for the optimal case, respectively. The energy consumption of the battery for the nominal case is given by experimental acquisitions, as described in Section 3. If $E_{bat,opt} = E_{bat,nom}$, the eco-driving indicator will be $ECO_{Energy} = 1$. This implies that the driver achieves the minimum energy consumption possible on that particular trip.

In the sequel of this section, we will describe the evaluation of $E_{bat,opt}$ for any given vehicle trip.

2.2 Optimization Problem Formulation

The objective of the optimal control is to minimize the overall energy consumption of the vehicle, intended as battery discharge. The optimization horizon, or segment, is defined as the distance between two breakpoints, *i.e.* two geographical points separated by a known distance, at both of which the speed is imposed. In practice, the optimization horizon corresponds usually to the distance between two successive stops (*i.e.* imposed speed equal to zero). The degree of freedom that can be used to achieve the optimization objective is the vehicle speed. Therefore, the output of the optimal control is the sequence of speed values that would generate the lowest energy consumption, while moving the vehicle between the two breakpoints in a prescribed time T . Experimental acquisitions on non-controlled vehicles, collected in a database, give this prescribed time as the one corresponding to real-life driving conditions. The same experiments generate a nominal speed profile for each segment.

The formalization of this problem can be done using the following system description and constraints:

$$\begin{cases} \dot{d}(t) = v \\ \dot{v}(t) = f(v, u, d) \\ d(T_k) = D_k \\ v(0) = v_{i,k} \\ v(D_k) = v_{f,k} \\ v(d) \in \mathfrak{X}(d) \subset \mathbb{R} \\ u(d) \in \mathfrak{U}(d) \subset \mathbb{R} \end{cases} \quad (23)$$

where $v(d)$ is the vehicle speed, d is the distance traveled and $u(d)$ is the control variable defined in Equations (15) and (16). The function $f(v, u, d)$ is given by Equation (1). T_k is the time duration of the segment k , D_k its length, v_i and v_f are the initial and the final speed of each segment, respectively. The sets:

$$\mathfrak{X}(d) = \{v_{min}(d) < v(d) < v_{max}(d)\} \quad (24)$$

and

$$\mathfrak{U}(d) = \{-1 < u(d) < 1\} \quad (25)$$

represent the constraints on the state and the control input, where $v_{min}(d)$, $v_{max}(d)$ are the minimum and maximum speed limits. This formulation makes use of reference profiles, which are assumed to be known.

Dynamic programming [10] is used to obtain the optimal solution to the 1-state problem. The implementation makes use of the open-source function *DPM*, developed at ETH-Zurich [11]. This approach is similar to what was proposed in [12] where we use only the speed as a state, and consider the distance as the independent variable: in this case, the distance constraint is automatic (horizon length), while the time constraint is to be enforced separately. To do so, a tunable coefficient β is used to treat the time constraint as an additional contribution to the optimization criterion [6].

2.3 Energy Minimization for a Simple Travel

The objective of the simulations shown in this paper is to demonstrate the potentiality of the approach proposing a method that will serve as the basis for future online implementation.

To illustrate the characteristics of the solutions found, two baseline cases are first considered. For a given time duration $T = 25$ s, first a relatively short distance $D = 100$ m (case A), then a relatively long distance $D = 200$ m (case B) are considered. In both cases, $v_i = v_f = 0$, that is, the segment considered is between two vehicle stops.

The optimal solution for the case A is shown in Figure 10. The trace of the control variable, the motor torque, clearly shows that the optimal trajectories are made of four different phases. In the first phase, the torque decreases from a maximum value (that is lower than the maximum motor torque in the case A) to the zero value. Correspondingly,

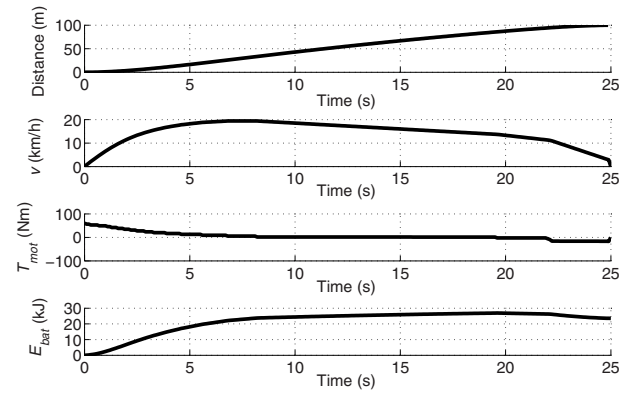


Figure 10
Optimal solution with $T_k = 25$ s and $D_k = 100$ m (case A).

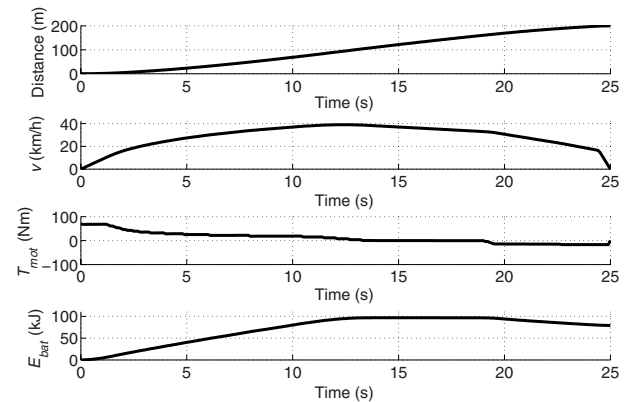


Figure 11
Optimal solution with $T_k = 25$ s and $D_k = 200$ m (case B).

the vehicle speed increases and reaches its maximum (lower than the maximum vehicle speed in the case A). In the second phase, the motor torque is around zero and the vehicle speed decreases due to the drag forces. In a short third phase, the motor torque decreases to negative values (regenerative braking), until a minimum value is reached, corresponding to the limits of the machine in generator mode. In the fourth phase, the motor torque is constant at its minimum value and the vehicle keeps decelerating. A fifth phase is barely visible at the very end of the mission, where the friction brakes are activated and the vehicle decelerates to its complete stop. The battery energy consumed amounts to 23.54 kJ.

In the case B, see Figure 11, the optimal trajectories are characterized by an additional initial phase, with the motor torque saturated to its maximum value. Then a decreasing torque phase, although less linear than in the case A is observed, followed by a null torque phase, a decreasing torque phase, a minimum torque phase and, finally,

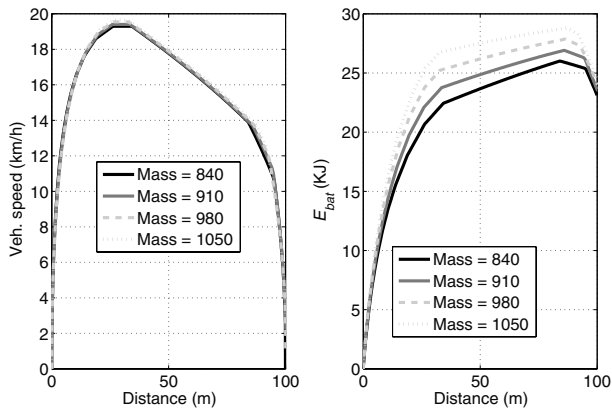


Figure 12

Optimal energy with different mass vehicle.

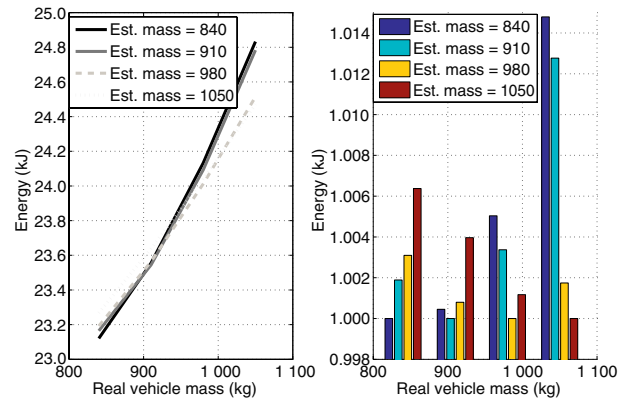


Figure 13

Optimal energy with different mass vehicle.

a friction braking phase. The vehicle speed varies accordingly, still remaining below its maximum admissible value.

2.4 Robustness

In this section, we study the robustness of the optimal solution presented above with respect to the different parameters changes of the vehicle model. As we already shown, the solution of the *DP* is based on a mathematical model representing the system. Therefore, any perturbation of the physical parameters of the system may impact the optimal solution. We are particularly interested by:

- the mass of the vehicle M ;
- and the parameters a , b , and c of the vehicle model.

Therefore, we study the impact of these parameter's variations on the optimal speed trajectory and on the energy consumption. To do that, we define the following constraints of the optimization problem:

- the time duration of the segment is 25 s;
- the length of the segment is 100 m;
- the initial and final speed are zeros.

Figure 12 shows the optimal speed profile and the energy consumed for different values of M . We can observe that the optimal speed has the same behavior for the four cases and the energy consumed is proportional to the mass of the vehicle M . For a 25% increase in the vehicle mass, the consumption is increased by 5.5%. In this case, the estimated value of the mass vehicle used in the controller is equal to the real one. In Figure 13, we present the energy consumed by the vehicle to realise different speed optimal profiles for different mass values. These profiles are obtained with different estimated values of M . This will indicate the impact of overestimating or underestimating the value of the vehicle mass while solving the optimization problem on the energy

consumed. The y -axis of the right side of Figure 13 is defined as the norm of the energy with respect to the optimal one. Therefore, we can observe that the optimal solution *i.e.*; that corresponds to minimum energy consumption is obtained when the estimated value of the mass is equal to the real vehicle mass.

For example, we can observe that, if the real vehicle mass is equal to 1 050 kg the minimal energy consumed is obtained of course if we use this value while solving the optimization problem. However, if we underestimate this value ($M = 840$ kg) while generating the optimal speed profile, the loss in energy is only 1.45% with respect to the optimal profile computed while using the correct value of the mass. Even lower errors are obtained for different values of the mass.

Figures 14 and 15 show the same simulation tests while varying the value of the parameter a of the vehicle model. We recall that this parameter represent the mechanical friction on the wheel. As we can observe, increasing the friction on the wheel implies more energy consumption. By varying the value of a by $\pm 50\%$, we have $\pm 33\%$ in energy consumption, approximately. However, even large errors in the estimated values of a induce differences lower than 5% with respect to the optimal energy profile.

Finally, the same simulations are done while varying the value of b and c of the vehicle model. See Figures 16–19. These parameters correspond to the rolling and the aerodynamic frictions, respectively. However, in this case, we increase the traveled distance to $D_k = 200$ m while maintaining the same time travel. This is because, these parameters are multiplied by the vehicle speed in the model and in order to see clearly their impact on the speed profile and the energy, we increase the average speed. By varying the value of b and c by $\pm 50\%$, we have $\pm 8\%$ and $\pm 6\%$, respectively.

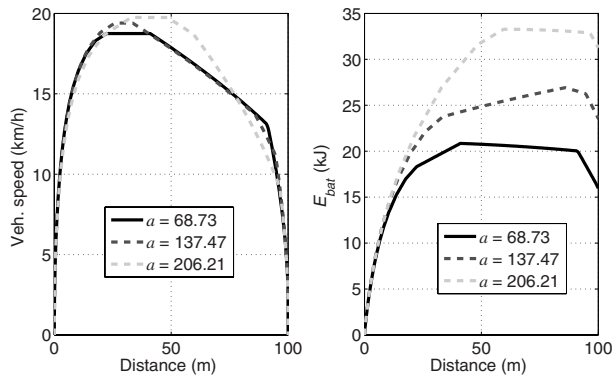


Figure 14

Optimal energy with variation of the parameter a of the vehicle model.

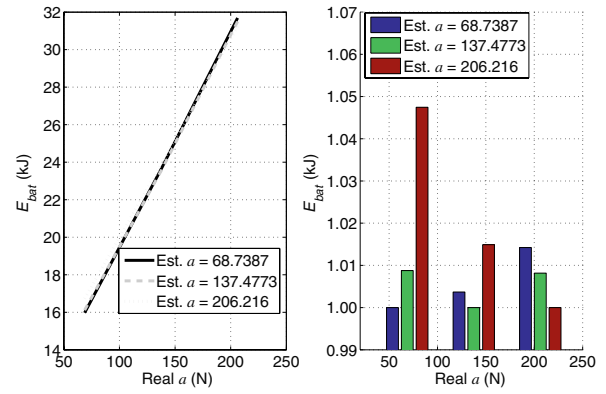


Figure 15

Optimal energy with variation of the parameter a of the vehicle model.

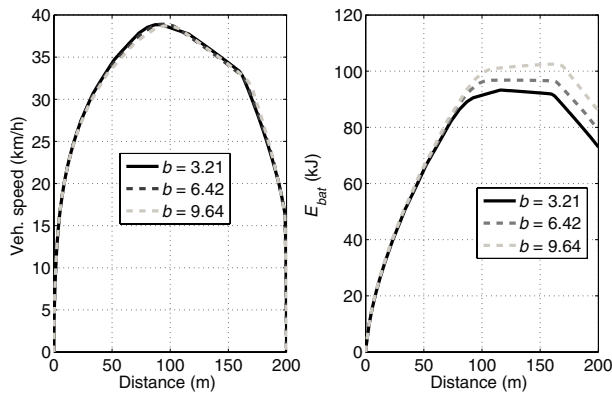


Figure 16

Optimal energy with variation of the parameter b of the vehicle model.

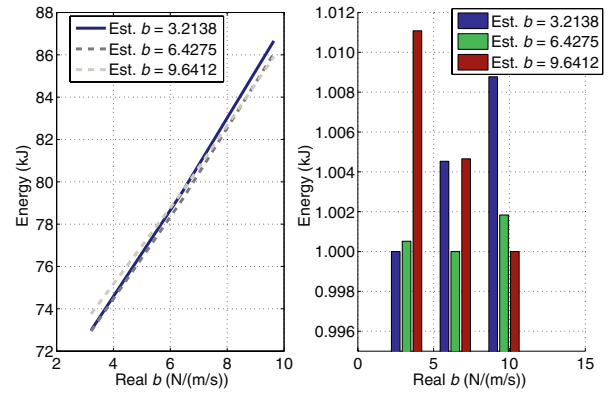


Figure 17

Optimal energy with variation of the parameter b of the vehicle model.

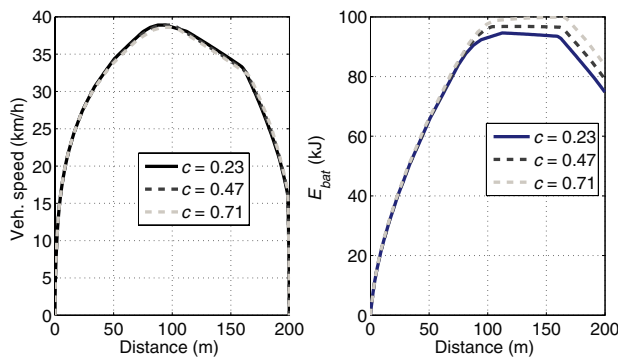


Figure 18

Optimal energy with variation of the parameter c of the vehicle model.

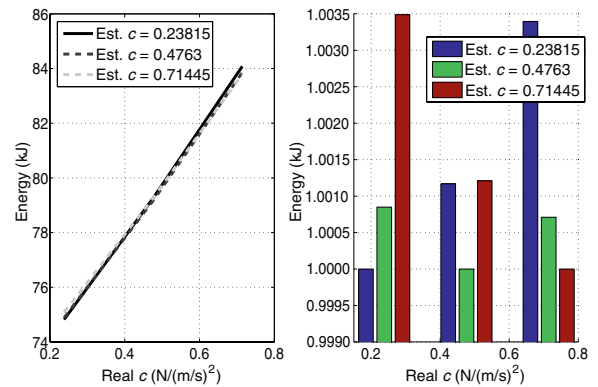


Figure 19

Optimal energy with variation of the parameter c of the vehicle model.

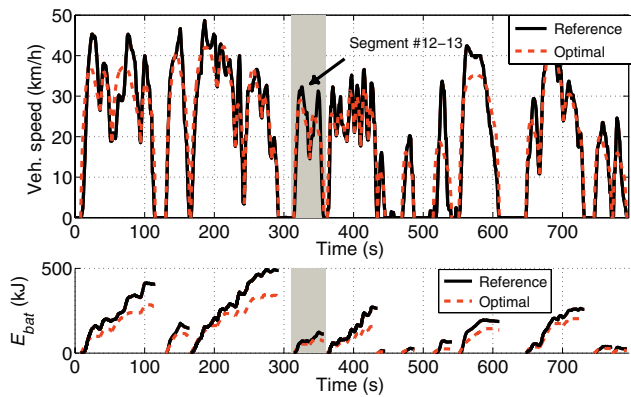


Figure 20

Optimal trajectory compared to the nominal case.

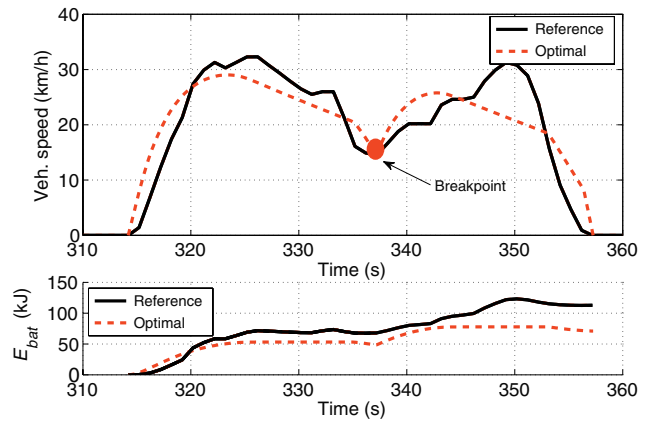


Figure 21

Optimal trajectory for the segments number #12 and 13 (shaded area in Fig. 20), compared to the nominal case.

The optimal speed profiles have the same behaviors in both cases. Large errors on the estimated values of b and c induce less than 1% difference with respect to the optimal case.

3 EXPERIMENTAL ILLUSTRATION

In this section, the optimal speed profiles obtained as described in Section 2.3 are compared to nominal trips, *i.e.* real-world experimental data, measured by driving the vehicle in urban driving conditions. Some of these data, *i.e.* those not directly available, have been post processed using the backward model of Section 1. The terminal conditions and speed limits of the optimal trajectory match the nominal data.

A total of 828 trips have been recorded, for a total distance of 1 540 km. The average speed is of 17 km/h, which is typical of urban driving conditions. The total amount of energy consumed is 311 kWh, which corresponds to the complete discharge of 21 batteries. An example trajectory is shown in Figure 20. The figure refers to a 4.57 km trip, subdivided into 28 segments, identified as sections between two minima in the speed profile. Vehicle speed and battery energy (cumulative discharge) are shown as a function of time. The distance traveled and the total time to complete the trip are identical between the reference and the optimal trajectory, thanks to the constraints introduced in the problem formulation. However, the optimal trajectory allows to reduce the overall energy consumption by a sensible amount, thanks to a better choice of the speed value at each instant. In order to better show the behavior of the optimal profile in comparison with the nominal, the segments #12 and 13 (shaded in Fig. 20) are magnified in Figure 21, where the same quantities are plotted.

The optimal trajectory consists in a smoother acceleration and lower peak speed, which reduces the peak power demand and therefore, the overall energy consumption.

The overall eco-driving indicator (22) of the whole trip is $ECO_{Energy} = 69.03\%$ where $E_{bat,nom} = 1\,945.9$ kJ and $E_{bat,opt} = 1\,343.4$ kJ. Table 2 shows the indicator ECO_{Energy} for the different segments of the trip. As the table clearly shows, the values of ECO_{Energy} are always lower than 85% and often lower than 70%. This means that the potential energy saving that could be achieved with appropriate eco-driving techniques is substantial for this trip. The results obtained for other trips confirm this assertion.

TABLE 2

Eco-driving indicator of the optimal trajectory compared to the nominal case for the first 13th segments

Seg. #	ECO_{Energy} (%)	Distance (m)	Average speed (m/s)
1	69.70	234.04	30.09
2	67.6	146.52	31.02
3	71.6	364.47	32.00
4	66.7	153.54	26.32
5	66.7	283.97	30.06
6	82.7	373.45	35.38
7	80.0	259.18	35.88
8	67.6	81.50	22.56
9	70.6	207.88	29.93
10	69.7	100.73	25.90
11	69.1	38.65	13.91
12	71.4	146.01	22.85
13	62.9	112.26	20.20

CONCLUSIONS

The potentiality for saving energy by optimizing the speed trajectory is demonstrated in this paper. A relatively small change in the driver's behavior (which could be suggested by an appropriate interface) could lead to significant energy savings.

This potential has been evaluated with respect to optimal speed trajectories. The optimization procedure that is presented is only suitable for an offline use. The next steps of this work will include the development of a driver-assistance system oriented to optimal eco-driving. To do so, the same optimal control problem formulation described in this paper will be used, however, different solving techniques will be necessary in order to allow for an online implementation.

ACKNOWLEDGMENTS

This work was done within the project VME (Ville, Mobilité, Énergie) with the collaboration of the LE2I Laboratory UMR-CNRS (<http://le2i.cnrs.fr>) and VULOG (<http://www.vulog.fr>). It has been partially supported by the French Environment and Energy Management Agency (Ademe).

REFERENCES

- 1 Sato S., Suzuki H., Miya M., Iida N. (2010) Analysis of the Effect of Eco-driving with Early Shift-up on Real-world Emission, SAE Paper 2010-01-2279.
- 2 Luu H.T., Nouvelière L., Mammari S. (2010) *Dynamic programming for fuel consumption optimization on light vehicle*, IFAC Advances in Automotive Control, Munich.
- 3 Sciarretta A., Guzzella L. (2005) Fuel-Optimal Control of Rendez-vous Maneuvers for Passenger Cars, *Automatisierungstechnik* **53**, 244-250.
- 4 Stoicescu A.P. (1995) On Fuel-Optimal Velocity Control of a Motor Vehicle, *Int. J. Vehicle Design* **17**, 229-256.
- 5 Petit N., Sciarretta A. (2011) Optimal drive of electric vehicles using an inversion-based trajectory generation approach, *18th IFAC World Congress*, Milano, Italy, 28 August-2 September.
- 6 Hellstrom E., Ivarsson M., Aslund J., Nielsen L. (2009) Look-ahead control for heavy trucks to minimize trip time and fuel-consumption, *Control Eng. Pract.* **17**, 245-254.
- 7 Guzzella L., Sciarretta A. (2007) *Vehicle propulsion systems. Introduction to modelling and optimization*, Springer-Verlag, 2nd edition, Berlin, Heidelberg.
- 8 Maes J., Melkebeek J.A. (2000) Speed-sensorless direct torque control of induction motors using an adaptive flux observer, *IEEE Trans. Ind. Appl.* **36**, 778-785.
- 9 Holtz J., Thimm T. (1991) Identification of the machine parameters in a vector-controlled induction motor drive, *IEEE Trans. Ind. Appl.* **27**, 1111-1118.
- 10 Bellman R., Dreyfus S. (1962) *Applied dynamic programming*, Princeton University Press, Princeton, NJ.
- 11 Sundstrom O., Guzzella L. (2009) A generic dynamic & programming matlab function, *IEEE Control Applications Intelligent Control*, 8-10 July, pp. 1625-1630.
- 12 Dib W., Serrao L., Sciarretta A. (2011) Optimal Control to Minimize Trip Time and Energy Consumption in Electric Vehicles, *Vehicle Power and Propulsion Conference (VPPC)*, 6-9 September.

*Final manuscript received in April 2012
Published online in September 2012*

Copyright © 2012 IFP Energies nouvelles

Permission to make digital or hard copies of part or all of this work for personal or classroom use is granted without fee provided that copies are not made or distributed for profit or commercial advantage and that copies bear this notice and the full citation on the first page. Copyrights for components of this work owned by others than IFP Energies nouvelles must be honored. Abstracting with credit is permitted. To copy otherwise, to republish, to post on servers, or to redistribute to lists, requires prior specific permission and/or a fee: Request permission from Information Mission, IFP Energies nouvelles, fax. +33 1 47 52 70 96, or revueogst@ifpen.fr.